Proceedings of ITC/ISHW2007

Analysis of MHD stability in high-β plasmas in LHD

Noriyoshi NAKAJIMA$^{1)}$, Satoru SAKAKIBARA$^{1)}$, Kiyomasa WATANABE$^{1)}$, Stuart HADOSON$^{2)}$,
and Cris HEGNA$^{3)}$

$^{1)}$*National Institute for Fusion Science, 322-6 Oroshi-cho, Toki 509-5292, Japan*
$^{2)}$*Princeton Plasma Physics Laboratory, PO Box 451, Princeton, NJ 08543, USA*
$^{3)}$*Department of Engineering University of Wisconsin-Madison, WI 53706, USA*

()

Up to now, theoretically idealized MHD equilibria reflecting experimental conditions have been used in order to examine the ideal MHD stability. This approach has been useful from the aspect of investing general properties of the ideal MHD stability. Since the properties of a three dimensional MHD equilibirium with large Shafranov shift significantly change by the pressure profile, the current profile, and the boundary condition, however, ideal MHD stability analysis based on theoretically idealized MHD equilibria is considered not to be enough to investigate the proper MHD atbility of experimentally obtained MHD equilibria. Indeed, it is shown that ideal MHD stability based on the realistic reconstructed MHD equilibrium with fine structures is different from that based on the theoretically idealized MHD equilibrium. Especially, it is firstly reported that high-*n* ballooning modes are destabilized in the magnetic well region with tokamak-like magnetic shear.

Keywords: high-*n* ballooning modes, LHD

DOI: 10.1585/pfr.1.001

1 Introduction

In three-dimensional configurations, the confinement region is surrounded by the stochastic magnetic field lines related to magnetic islands or separatrix, leading to the fact that the plasma-vacuum boundary is not so definite compared with tokamaks that the various modulations of the plasma-vacuum boundary will be induced around the stochastic region by synergetic effects between a transport around the stochastic region and a large Shafranov shift of the whole plasma or a large Pfirsch-Schluter current, in especially high-β operations.

To examine such modulation effects of the plasma boundary on MHD instabilities, high-β plasmas allowing a large Shafranov shift or a large Pfirsch-Schluter current are considered in the inward-shifted LHD configurations with the vacuum magnetic axis R_{ax} of 3.6 m, so that it has been found that the free boundary motion of MHD equilibrium or the whole plasma outward-shift due to a large Pfirsch-Schluter current has significant stabilizing effects on ideal MHD instabilities, leading to partially resolving the discrepancy on MHD stability between experimental results and theoretical analyses [1].

Although experimental aspects on the boundary, the pressure profile, and the current condition are included in the equilibria used in Ref.[1], such equilibria are still theoretically idealized judging from the experimental point of view [2]. Thus, it is needed to use equilibria which are more relevant to the experimental conditions, in order to more clarify MHD stability in planar axis Heliotron configuration with a large Shafranov shift like LHD. The purpose of the present research is to clarify MHD stability especially in IDB-SDC plasma or high-β plasma of LHD by comparing between theoretically idealized MHD equilibria and experimentally reconstructed MHD equilibria. For such a purpose, especially, high-*n* ballooning local mode stability analysis is performed, because such local mode analysis does not need whole information of MHD equilibrium. The precise information of MHD equilibrium near the plasma periphery is not needed, once the core MHD equilibrium is consistently reconstructed to experimental conditions. This research might lead to more deeper understanding of MHD equilibrium and stability in the planar axis Heliotron configuration with a large Shafranov shift like LHD.

2 in theoretically idealized MHD equilibria

In order to clarify dependence of the stability properties of the ideal high-*n* ballooning on MHD equilibrium, firstly, high-*n* ballooning stability analyses are performed for theoretically idealized MHD equilibria in the inward-shifted vacuum configuration with $R_{ax} = 3.75$ m.

2.1 in currentless MHD equilibria with peaked pressure profile

The properties of currentless MHD equilibria with a peaked pressure profile; $P(s) = P_0(1^s)^2$, under the fixed boundary condition are shown in Fig.1, where s is the normalized toroidal flux. As β increases by using P_0,

---

author's e-mail: nakajima.noriyoshi@nifs.ac.jp

tokamak-like magnetic shear is created near the magnetic axis. Although the magnetic hill still remains near the plasma periphery, the Mercier stability in the magnetic hill region is improved as β increases. Boundary between magnetic well and hill exists in helical-like maggnetic shear region. The corresponding normalized growth rates of high-n ballooning modes are shown in Fig.2. High-n ballooning modes are destabilized in the peripheral magnetic hill region with helical-like magnetic shear. As β increases, properties of the high-n ballooning modes change from helical-like ones with strong magnetic field line dependence to tokamak-like ones with weak magnetic field line dependence. Helical-like high-n ballooning modes become unstable only near the magnetic field line with $\alpha = \zeta - q\theta = 0$ where the local magnetic curvature is baddest. On the other hand, tokamak-like high-n ballooning modes become unstable independent of the magnetic field line, even in the magnetic field line with $\alpha = \pi/M$ (M is the toroidal field period of the MHD equilibrium) where the local magnetic curvature is locally good.

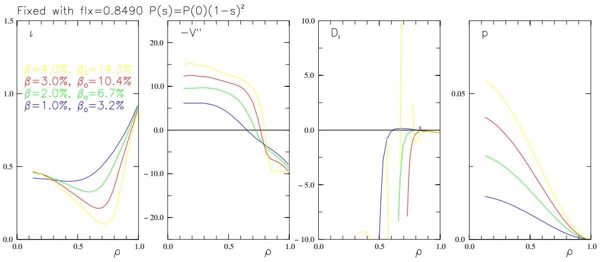

Fig. 1 β-dependences of the rotational transform , magnetic well and hill $-V$”, and Mercier criterion D_I with pressure profile P in currentless MHD equilibria with the peaked pressure profile under the fixed boundary condition.

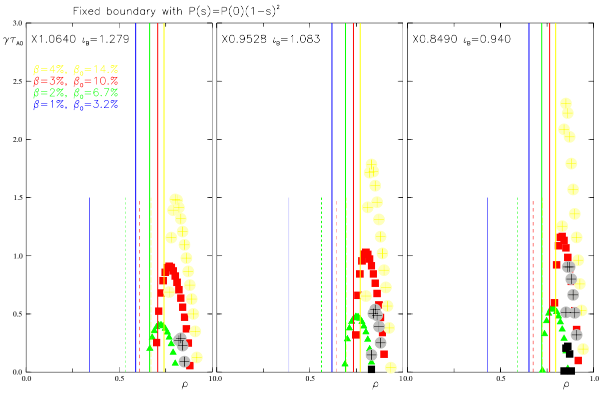

Fig. 2 β-dependence of the normalized growth rates $\gamma\tau_{A0}$ for three different plasma volumes. The most right column corresponds to 1

In order to investigate effects of the boundary condition, the MHD equilibria are created under the free boundary condition. In Fig.3, the properties of currentless MHD equilibria under the free boundary condition is shown. Although the β-dependences of the magnetic shear, magnetic well, and Mercier stability in free boundary equilibria are qualitatively similar to those in fixed boundary equilibria, change of iota in free boundary equilibrium is more significant than that in fixed boundary equilibrium, and formation of magnetic islands is suggested in shearless region judging from the spikes of D_i. The spike comes from the divergence of the Pfirsch-Sch”ulter current indicating existence of the magnetic island. The corresponding normalized growth rates of high-n ballooning modes are shown in Fig.4. Most significant differences between fixed boundary equilibria and free boundary equilibria are that helical-like ballooning modes destabilized in the magnetic hill region with helical-like magnetic shear extend to the magnetic well region with tokamak-like magnetic shear. Since ballooning formalism breaks near shearless region, the global mode analysis migh be needed for precise stability.

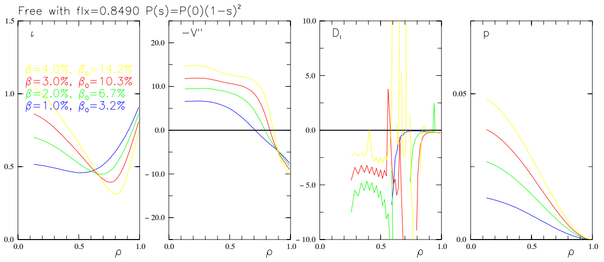

Fig. 3 β-dependences of the rotational transform , magnetic well and hill $-V$”, and Mercier criterion D_I with pressure profile P in currentless MHD equilibria with the peaked pressure profile under the free boundary condition.

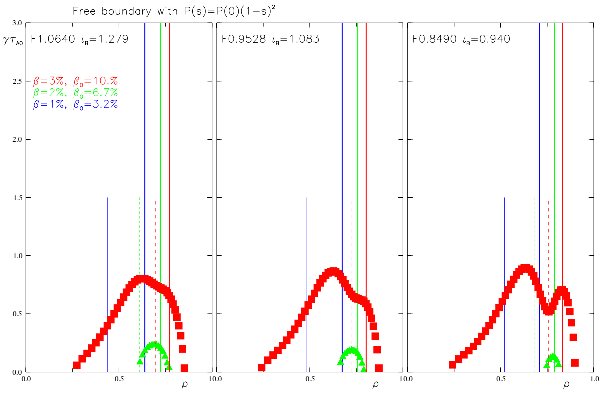

Fig. 4 β-dependence of the normalized growth rates $\gamma\tau_{A0}$ for three different plasma volumes. The most right column corresponds to 3

2.2 in currentless MHD equilibria with broad pressure profile

In order to investigate effects of the pressure profile, the currentless MHD equilibria are made with a broad pressure profile; $P(s) = P_0(1 - s^2)^5$. In Fig.5, the properties of the currentless MHD equilibrium with the broad pressure profile under the fixed boundary is shown. The steep pressure gradient near the plasma periphery coming from the broad pressure prifile makes magnetic hill region narrow.

The corresponding normalized growth rates are indicated in Fig.6. As well as the MHD equilibria with peaked pressure profile, high-n ballooning modes are destabilized in the peripheral magnetic hill region with helical-like magnetic shear. As β increases, properties of the high-n ballooning modes change from helical-like ones with strong magnetic field line dependence to tokamak-like ones with weak magnetic field line dependence.

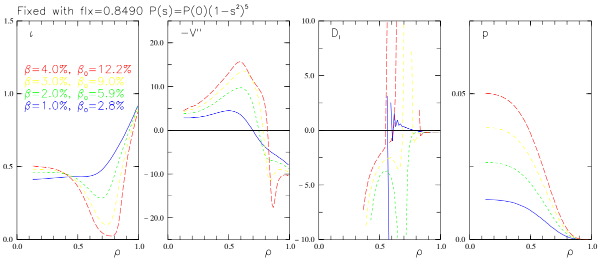

Fig. 5 β-dependences of the rotational transform , magnetic well and hill $-V$”, and Mercier criterion D_I with pressure profile P in currentless MHD equilibria with the broad pressure profile under the fixed boundary condition.

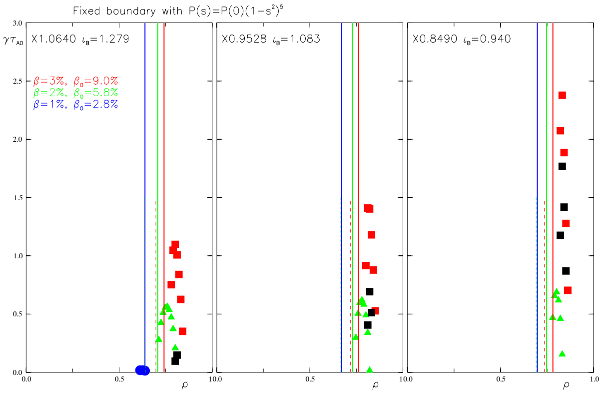

Fig. 6 β-dependence of the normalized growth rates $\gamma\tau_{A0}$ for three different plasma volumes. The most right column corresponds to 5

The effects of the free boundary are shown in Figs.7 and 8 for currentless MHD equilibria with a broad pressure profile. The differences between fixed boundary and free boundary are same as the case of currentless MHD equilibria with peaked pressure profile.

3 in reconstructed MHD equilibria

In this section. the stability of high-n ballooning modes is investigated in the reconstructed MHD equilibria.

The Fig.9 denotes the properties of both the reconstructed MHD equilibrium and the variations corresponding to IDB-SDC plasma in the standard configuraion with R_{ax} = 3.75m. The corresponding normalized growth rates are shown in Fig.10. The behaviors of all quantities of equilibrium and stability are similar to those in the theoretically idealized MHD equilibria.

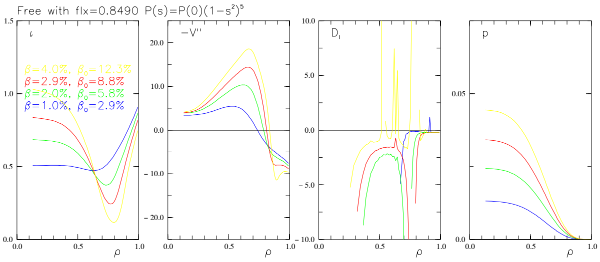

Fig. 7 β-dependences of the rotational transform , magnetic well and hill $-V$”, and Mercier criterion D_I with pressure profile P in currentless MHD equilibria with the broad pressure profile under the free boundary condition.

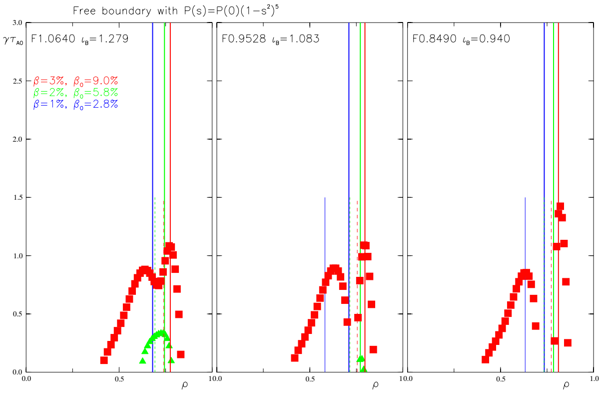

Fig. 8 β-dependence of the normalized growth rates $\gamma\tau_{A0}$ for three different plasma volumes. The most right column corresponds to 7

The properties of the reconstructed MHD equilibrium corresponding to IDB-SDC plasma in the outward-shifted vacuum configuraion with R_{ax} = 3.85m are denoted in the upper row of Fig.11. The corresponding normalized growth rate is shown in the left column of Fig.**??**. The most significant feature of stability of the high-n ballooning modes is that helical-like ballooning modes appear in the both magnetic hill region with helical-like magnetic shear and magnetic well region with tokamak-like magnetic shear. Moreover, high-n ballooning modes in the magnetic well region with tokamak-like magnetic shear are more tokamak-like ballooning modes than those in the magnetic hill region with helical-like magnetic shear, because the magnetic field lines where the mode is unstable are wider in the magnetic well region with tokamak-like magnetic shear than in the magnetic hill region with helical-like magnetic shear. As is understood from the pressure profile shown in upper row of Fig.11, the reconstructed pressure profile has fine structures, namely, slight stair-case like structures. Although those fine structures are not so significant, it is considered that such fine structure changes the stability criterion of the high-n ballooning modes through the balance between stabilization effect due to the local magnetic shear and destabilization effect due to the local magnetic curvature. High-n ballooning modes in the magnetic well region with tokamak-like shear might

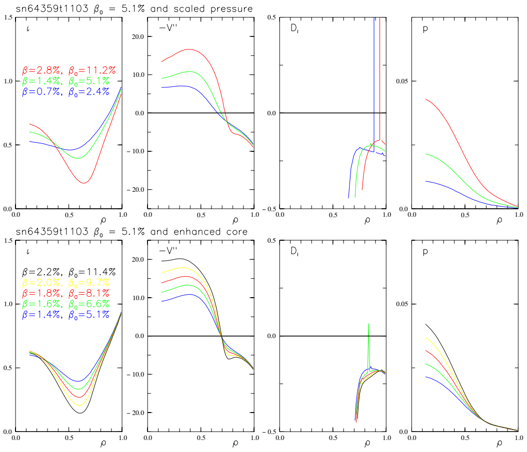

Fig. 9 β-dependences of the rotational transform , magnetic well and hill $-V$”, and Mercier criterion D_I with pressure profile P in reconstructed MHD equilibria and the variations in the stabdard vacuum configuration with R_{ax} = 3.75. The upper (lower) row includes the β-variations of whole (core) region.

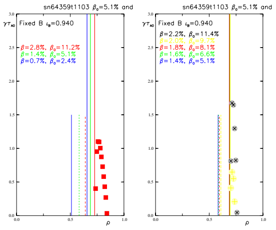

Fig. 10 β-dependence of the normalized growth rates $\gamma\tau_{A0}$ for three different plasma volumes. The left (right) column includes the β-variations of whole (core) region.

lead to core density collapse experimentally reported.

The properties of the reconstructed MHD equilibrium corresponding to high-β plasma in the inward-shifted vacuum configuraion with R_{ax} = 3.60m are denoted in the lower row of Fig.11. The corresponding normalized growth rate is shown in the right column of Fig.**??**. As well as the above case of IDB-SDC, fine structures of the pressure profile makes the significant change in the Mercier criterion, leading to the non-monotonic change in the normalized growth rate as os shown in the right column of Fig.**??**.

4 Summary

Up to now, theoretically idealized MHD equilibria reflecting experimental conditions have been used in order to examine the ideal MHD stability. This approach has been useful from the aspect of investing general properties of the ideal MHD stability. As is well know, however, the properties of a three dimensional MHD equilibirium with large Shafranov shift significantly change by the pressure profile, the current profile, and the boundary condition. Indeed, high-n ballooning stability is completely different between equilibria under fixed boundary and those under free boundary. Although free boundary equilibria are more stable than fixed boundary ones in the inward-shifted vacuum configuration with R_{ax} = 3.60m, free boundary equilibria are more unstable than fixed boundary ones in the standard vacuum configuration with R_{ax} = 3.75m. Moreover, it is shown that ideal MHD stability based on the realistic reconstructed MHD equilibrium with fine structures is different from that based on the theoretically idealized MHD equilibrium. Especially, it is firstly shown that high-n ballooning modes are destabilized in the magnetic well region with tokamak-like magnetic shear, which means that high-n ballooning stability is quite sensitive to MHD equilibrium. Stability analyses based on idealized MHD equilibria might not be enough to interpret experimental results on MHD stability. More extensive stability analyses based on reconstructed MHD equilibria will be needed.

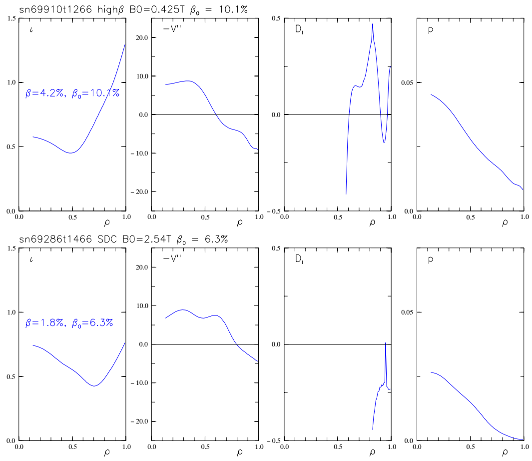

Fig. 11 β-dependences of the rotational transform , magnetic well and hill $-V$”, and Mercier criterion D_I with pressure profile P in reconstructed MHD equilibria. The upper (lower) row corresponds to the reconstructed equilibrium in the outward-shifted (inward-shifted) vacuum configuration with R_{ax} = 3.85 (3.60) m.

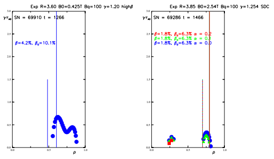

Fig. 12 β-dependence of the normalized growth rates $\gamma\tau_{A0}$. The left (right) column corresponds to the reconstructed equilibrium in the outward-shifted (inward-shifted) vacuum configuration with R_{ax} = 3.85 (3.60) m.

[1] N. Nakajima, et al., Nucl. Fusion **46** (2006) pp.177-199.

[2] K.Y. Watanabe, et al., Plasma Phys. Control. Fusion, **49** (2007) pp.605-618.